design of a V twin

by Simon Hughes

FILE	6356_SIMON_HUGHES_DESIGN_OF_A_V_TWIN_128469_855952238.DOCX (6.23M)		
TIME SUBMITTED	30-APR-2019 08:35AM (UTC+0100)	WORD COUNT	7199
SUBMISSION ID	105798384	CHARACTER COUNT	34973

2019

Analysis and design of a V configuration motorcycle engine.

UNIVERSITY OF WALES TRINITY SAINT DAVID
Simon Hughes
P147135
06/03/2019
M6X00417, Major project.
Malcolm McDonald.

2019

'This thesis is the result of the author's original research. It has been composed by the author and has not been previously submitted for examination which has led to the award of a degree.'

Signed: *Date:*

1 Table of Contents

2 Annotations 4

3 Abstract 5

4 Introduction 5

5 Engine analysis 6

5.1 Aprilia SXV 6

5.2 SV650 7

5.3 VFR400 8

5.4 Measurements 9

6 Designed engine 12

6.1 Manufacture considerations 16

6.2 Balancing 17

7 FEA 21

7.1 Mesh 25

8 Balance shafts 34

8.1 Vector calculations for a single cylinder 36

9 Centre of gravity 36

10 Metal treatments 38

10.1 Induction hardening 38

10.2 Pulse plasma nitriding 39

10.3 shot peening 39

10.4 diamond like coat 39

11 Further work 39

11.1 Head model 39

11.2 Engine cases and gearbox 40

11.3 Friction model 40

12 References 41

Figure 1 SXV550 (motorcyclespecs, 2019) 6
Figure 2 SV650 (motorcyclespecs, 2019) 7
Figure 3 VFR400 (motorcyclespecs, 2019) 8
Figure 4 SXV550 CAD model 10
Figure 5 SV650 CAD model 10
Figure 6 VFR400 CAD model 11
Figure 7 final design of new engine 15
Figure 8 450 v-twin first order inertia 17
Figure 9 450 v-twin second order inertia 18
Figure 10 450 v-twin total inertia 18
Figure 11 SXV550 total inertia 19
Figure 12 SV650 total inertia 20
Figure 13 VFR400 total inertia 20
Figure 14 Pressure by crank angle 22
Figure 15 Cylinder 2 Solidworks data points plot 23
Figure 16 Cylinder 1 Solidworks data points plot 24
Figure 17 Meshed crank 25
Figure 18 close view of big end journal and oil hole meshing 26
Figure 19 FEA stress concentration, compressive zone (von mises stress) 27
Figure 20 4130 steel material selection in Solidworks 28
Figure 21 4340 steel material selection in Solidworks 28
Figure 22 Von Mises stress plot 29
Figure 23 FEA stress concentration, tensile zone (2nd principal stress) 30
Figure 24 Second principal stress plot 31
Figure 25 FEA Displacement 32
Figure 26 Displacement plot 33
Figure 27 vectors diagram 35
Figure 28 90-degree semicircle segment 36
Figure 29 COG polynomial plot 10mm base 37
Figure 30 COG polynomial plot 20mm base 37
Figure 31 steel phase diagram (Industrial Metallurgists LLC, 2019) 38

Table 1 measured and calculated values of analysed engines 12

2 Annotations

R – crank pin throw radius
L – length of conrod
M_{rec} – reciprocating mass
M_{rot} – rotational mass
X – distance from center of gravity to center of rotation of crank
P – pressure

Y – distance from center of gravity to center of rotation of balance shaft
M_{bal} – Balance shaft offset mass

CC – cubic centimeters

C.A.D – computer aided design

3 Abstract

Much of modern engine design is done through the experience of senior engineers, though all this experience is backed by the success of the engines that are designed, this report will try to work on a possible numerical way to design the internal components of an engine.

Several engines were analysed to create the numerical model, from which any engine can be designed, the engines looked at are an Aprilia SXV550, a Suzuki SV650 and a Honda VFR400 and they are all engine that have a V configuration.

Using the numerical model created an engine will be designed, the numerical model will be created in excel and linked to several different designed parts in Solidworks, this will confirm the validity of the model and whether an engine can be designed from a purely numbers standpoint.

To back up the numerical methods used an FEA will be carried out on the finished parts to test how well the equations have worked. This FEA will also give an indication on what can be changed in the numerical model, as results of stress and deflection will be analysed.

Surface treatments will be given a passing explanation due to their individual complexities and variances in their own area.

4 Introduction

Internal combustion engines have been one of the many driving forces behind modern society for some years, this is due to their convenience and relatively small form factor compared to the size of other forms of power plants, such as electric vehicles which when are a comparable size and mass have much less range.

Most race series that use a 450cc motor use a single cylinder, this is great for torque, but top end power suffers, using a twin cylinder engine gives this better top end but loses some percentage of the torque a single cylinder engine offers.

The engine that is being designed is specifically for a Supermoto, so higher end power is a benefit, as the track the motorcycle will be ridden on is not as demanding of the lower end torque. As SuperMoto's usually get to speeds in excess of 80mph top end power is much needed in the sport, for some smaller track though this can be somewhat detrimental.

5 Engine analysis

When choosing what motorcycles to analyse the author had a specific set of criteria that need to be met, one being that they all had to have an engine that was in a v configuration, the angle of the v was not important. The second being that components were available to precisely measure, and finally they all had to be of a similar capacity, this final need was not totally met as the engines chosen were a 650cc, 550cc and a 400cc. this will give a large variance in the number outputs of each engine.

When analysing the engines from the chosen motorcycles there had to be an assumption made that all the engines were running at a peak cylinder pressure of around 80bar, this assumption is need as there is no pressure data available for any of the engines.

5.1 Aprilia SXV



Figure 1 SXV550 (motorcyclespecs, 2019)

The Aprilia SXV is a race bred motorcycle made by Aprilia from 2006 till 2011, it was produced in two different styles and two different engine capacity's, the first being a

motocross bike and second being a Supermoto, with both being available in a 450cc and a 550cc version.

The main problem that occurred with this motorcycle was that it had a very short maintenance cycle, this meant that if the engine wasn't maintained on a ride by ride basis the likelihood of bearing failure increased greatly. One other semi common problem for the larger capacity variant was the crank snapping, both problems could have several different reasons for occurring, one likely failure reason could be under oiling of the big end bearings and another could come from a design problem of the engine in the form of the 550cc engine having the same crank and bearings as the 450cc engine, only the conrod, piston and cylinder liners were changed, meaning that the forces from combustion might be greater, therefor putting more stress on the crank and bearings.

The engine in the SXV engine is a 77-degree v twin, which produces 70 horsepower.

5.2 SV650



Figure 2 SV650 (motorcyclespecs, 2019)

2019

The Suzuki Sv650 is a motorcycle that has shown its reliability throughout its production life, first manufactured in 1999 and ending production in 2017 only to be brought back again in late 2018 early 2019.

The engine in the SV 650 is v-twin with a 90-degree V angle, producing 72 horsepower.

Though not a race orientated motorcycle many amateur races use them in certain race series. Only when modifications to the engine start to be made do the engines run into problems. The most common is bearing failure, along the conrods being snapped, these problems are to be expected when the power output of the engine starts to be increased beyond what it was designed to produce

5.3 VFR400



Figure 3 VFR400 (motorcyclespecs, 2019)

Though not a V-twin the VFR400 was chosen due to it being in a v configuration, also with having four cylinders the individual cylinder sizes are much smaller than the other two

motorcycles, this means that the data retrieved from the measurement and calculations will be much smaller too, therefore care must be taken when comparing it to the others.

The engine in the VFR400 is a V-four with a 90-degree v angle producing 59 horsepower.

Like the SV650 the VFR400 had a long-lasting engine, this could be in part due to its small cylinder capacity and lower forces in the engine. Though not a large capacity motorcycle, RVF400 variant still ran in many race series including the isle of man TT and the north west 200. (simonevans, 2019)

5.4 Measurements

When analysing the selected engines, physical components had to be sourced, the parts collected were the crank, conrod, gudgeon pin and piston. The only exceptions to the parts collection were the SXV550 piston and gudgeon pin, the weight which was most important was found on the Aprilia forum. (thecunningham, 2019)

The first thing to be collected was the mass of all the individual components, this was done using a precision scale and recorded in excel. The radius of the of the crank pin throw was also measured. Once this set of figures are gained a measure of the balance can then be calculated.

$$M_{rot} = \frac{1}{3} \times conrod\ weight$$

$$M_{rec} = \frac{2}{3} \times conrod\ weight + piston\ mass + gudgeon\ pin\ mass$$

$$balancing\ force = \left(2 \times M_{rot} + \left(\frac{M_{rec}}{2}\right)\right) \times R)$$

$$X = \frac{M_{rec} \times R}{crank\ mass}$$

Many measurements had to be taken from the physical components obtained to create the following CAD models, these included many superficial measurements to imitate the visual aspect of each component. To make sure the CAD models were accurate the measurement of crank balance was used to validate the accuracy.

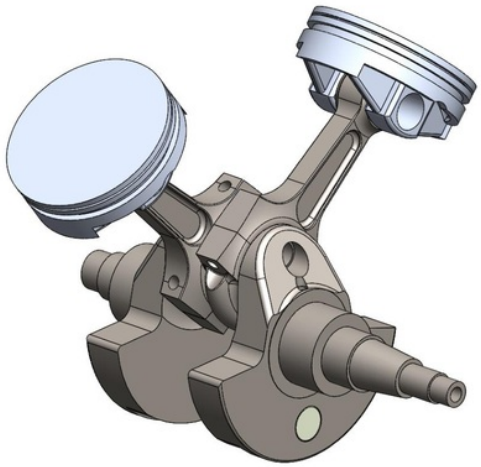


Figure 4 SXV550 CAD model

The pistons in the CAD model for the SXV550 have very little detail on them as the author had no access to the real item to measure properly, though this being the case information on the weight was obtained online to be used in the calculations portion of the work carried out. The balancing of the SXV crank in Solidworks did not work initially, this was quickly solved by finding out what the weights pressed into the crank were made of.

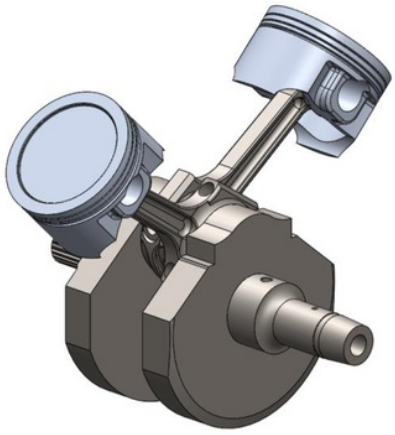


Figure 5 SV650 CAD model

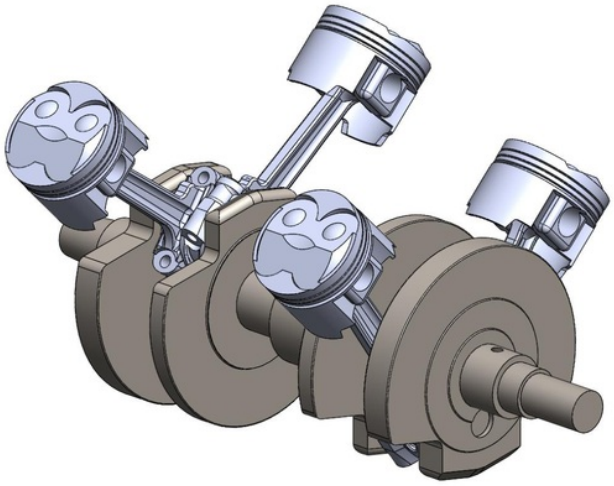


Figure 6 VFR400 CAD model

As can be seen in figures 4, 5 and 6 there is a large variance in the overall design of each of the analysed engines. From inspecting each of the different part the author has noted that the VFR and SV have very little machining on the cranks, but the SXV has a fully machined crank apart from some small area neat the big end journal.

There are two different types of VFR crank, on as pictured in figure 6 and the other which has both big end journals on the same side of the crank, the second type of crank comes from the VFRs twin the RVF400, this variant was the more race orientated version of the pair.

The following table lists the majority of what was measured and calculated in each of the three engines, these ultimately lead to the big end shell pressure.

This figure is important because it shows that although the SXV has a smaller capacity then the SV the bearing pressure is somewhat higher, this could be the possible cause for the common bearing failure problem the motorcycle experiences, if a bearing that was designed for the 450cc variant was used in the 550 variant then the bearing would have a much higher chance of wearing through and failing, this could easily be solved by using a higher rated bearing.

	SXV 550		SV 650		VFR 400	
crank mass	2.887	Kg	5.425	Kg	1.5435	Kg
crank pin throw	0.03032	m	0.031	m	0.0229	m
bob mass	0.69467	Kg	1.133	Kg	0.455	Kg
reciprocating mass	0.30133	Kg	0.431	Kg	0.199	Kg
rotating mass	0.19667	Kg	0.351	Kg	0.128	Kg
conrod mass	0.295	Kg	0.347	Kg	0.192	Kg
two thirds	0.19667	Kg	0.231	Kg	0.128	Kg
one third	0.09833	Kg	0.116	Kg	0.064	Kg
piston + pin mass	0.203	Kg	0.315	Kg	0.135	Kg
conrod length	0.0935	m	0.094	m	0.1	m
CoG	0.0072	m	0.00636	m	0.00636	m
piston diameter	0.0798	m	0.0803	m	0.0545	m
piston area	0.00500	m^2	0.005064	m^2	0.002333	m^2
pressure assumption	8000000	N/m^2	8000000	N/m^2	8000000	N/m^2
Fgas at peak	40011.575	N	40514.54	N	18662.63	N
Fnet @ assumed rpm	28842.661	N @10000	27099.917	N @ 9000	13397.82	N @ 12000
big end shell width	16	mm	16	mm	15	mm
big end shell diameter	35	mm	38	mm	30	mm
main journal diameter	38	mm	40.000	mm	30	mm
big end shell area	560	mm^2	608	mm^2	450	mm^2
big end shell pressure	51.5048	N/mm^2	44.5722	N/mm^2	29.77293	N/mm^2

Table 1 measured and calculated values of analysed engines

6 Designed engine

The engine being designed by the author is a V-twin that is suitable to enter all standard 450cc race categories.

There are several figures that are obtained from analysis the other engines, two of the ones need to start the whole calculation process are the mean piston speed and the max power RPM. Once a new figure for these two figures has been decided they are then used to work out the stroke of the engine, these two numbers essentially become the first building blocks of the engine being designed.

$$Stroke = \frac{mean\ piston\ speed \times 60}{2 \times \max power\ RPM} \times 1000$$

The next decision is what capacity the engine shall be, this is a completely personal choice.

$$Bore = \sqrt{\frac{cylinder\ capacity \times 4}{\pi \times \frac{stroke}{10}} \times 10}$$

Once the size of the new bore has been obtained an initial piston can be drawn up in a CAD package to give a mass to use later, Solidworks was used for this, when designing a piston there are many different factors that need to be considered, looking at the pistons from the other engines and several others that were available to the author an initial one was drawn up in Solidworks.

A Pmax of 80bar was also chosen for the new engine, this is the same as the assumed cylinder pressures for the analysed engines, this is all due to the author having a data set for a triumph three-cylinder 675cc. The triumph engine has 225cc per cylinder, this cylinder size is also the same as the engine being designed, therefor the decision was made that it would be appropriate to use this data to create a realistic FEA model.

A bearing shell material then needs to be chosen to determine a theoretical maximum pressure allowed on the big end bearing, this was done using the Mahle powertrain book, cylinder components, the material chosen was MAS16, which has a maximum rated pressure of 50Mpa. Due to this rated bearing pressure the maximum allowed pressure chosen by the author was 30Mpa, this is to allow for a factor of safety.

Choosing the rod width comes as an educated choice, too thin and it may not be strong enough, too thick and it would be unnecessarily heavy. This choice can be changed depending on the results of a finite element analysis. To carry on with the calculations the author used 20mm as a starting width.

One of the key results from the analysed engines is the R/L figure, this figure is obtained by dividing the crank pin throw radius by the length of the conrod, this figure is important as it defines the length of the conrod when compared to the throw of the crank.

Once a suitable R/L figure has been decided on a new conrod can be drawn up in CAD, this then allows another component of the reciprocating mass to be gained, leaving only the gudgeon pin.

Comparing the engines analysed earlier a gudgeon pin diameter can be decided on, this diameter can be change with the results of the FEA. Though there are some methods of calculating this dimension.

To calculate the big end journal diameter there are a couple of steps, the first step is to find the inertia force created by the reciprocating mass, this uses the reciprocating mass, the crank throw radius, the speed of the crank in radians and the particular angle the crank is at, the exact steps follow,

$$F_{inertia\ first\ order} = M_{rec} \times R \times \omega^2 \times \cos\theta$$

$$F_{inertia\ second\ order} = \frac{R}{L} \times M_{rec} \times R \times \omega^2 \times \cos 2\theta$$

$$F_{inertia\ total} = F_{inertia\ first\ order} + F_{inertia\ second\ order}$$

$$F_{net} = F_{gas\ peak} - F_{inertia\ total}$$

$$Big\ end\ diameter = \frac{F_{net}}{shell\ width \times big\ end\ allowed\ P_{max}}$$

The big end diameter uses the F_{net} figure calculated using the aforementioned inertia force, this is then divided by the width of the shell type bearing that the big end runs on, this width is slightly smaller than the rod width, this comes from looking at the other engines and seeing that the bearings have a chamfered edge, therefore reducing their width by up to 2mm.

The main diameter is calculated using the results from the analysed engines, this is done by finding the ratio between the big end journal and the main bearing journals sizes.

$$Main\ journal\ diameter = big\ end\ diameter \times big\ end\ to\ main\ ratio$$

Building in the 100% crank balance comes in the form of the user input crank web design, the crank web can be any shape, within reason, that the creator wants, if a design has already been decided on then finding X would be required, but if not then finding the balance force would be needed, both methods are shown in equation form below.

$$100\%\ balance = 2 \times \frac{M_{rot} + M_{rec}}{2} \times R$$

For the balance force equation, it starts with a 2, this is due to there being two cylinders on one big end journal, this means there is a need for two sets of the masses.

$$X = \frac{M_{rec} \times R}{crank\ mass} \times 1000$$

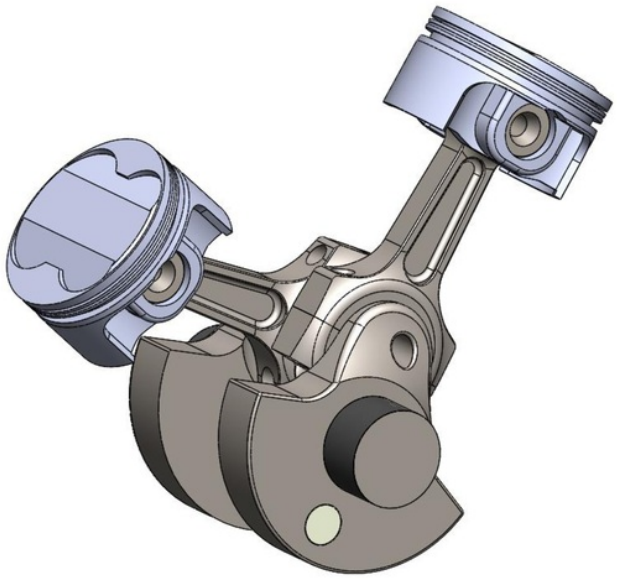


Figure 7 final design of new engine

The final design of the new engine is like the SXV in the fact the it is made to be as light as possible but still retain a 100% balance, as such the steel component of the balance is made under sized and supplemented with tungsten plugs, this means that the cranks outer most diameter can be smaller but still retain its 100% balance.

To finalize the design process the excel needed to be linked to Solidworks, this was done using design tables, this feature creates an internal excel document with named dimensions within the designed part, these dimensions can then be linked across to the workbook that all of the design calculations have been created in.

This linking process can be troublesome at times, since the calculations workbook, the CAD model and the design table must be open at the same time for changes to take effect. Another frequent problem encountered was when closing the design table Solidworks would lock the user interface, therefore not allowing the user to interact with anything except to close the program, this proved to be somewhat of a nuisance as changes made during the session were lost.

6.1 Manufacture considerations

There are several different ways that engine components can be manufactured. The components can be cast, forged, machined out of a billet of steel or aluminium or in more recent times compressed sintered metal powder. These processes give greatly different properties to the final products, but all share the same finishing methods. Materials can also give the components much different properties, steel is the most common material for cranks conrods and gudgeon pins, though there are many different grades of steel. Aluminium is normally only used in high performance engines that don't have a long life before a rebuild.

Cranks can be made using the casting, forging or billet methods. Each of these offers different properties to the final product. Cast cranks are slowly falling out of use in modern engines being replaced by forged cranks, this is due in part to the ease of forging a crank rather than casting it and the added strength that comes from the forging process. The billet method is normally only used in racing applications due to the high price of manufacture; this high price is due to the crank needing to have many hours of machining performed and the amount of waste material that is produced.

Conrods are conventionally made of steel but can be made of aluminium or even titanium when used in racing applications. The main downside of aluminium is that is doesn't have a great fatigue life, this would be fine for race engines but not for conventional road engines, titanium rods are particularly rare as they are costly but also because they have a larger in use stretch value that must be accounted for, if this is not accounted for the engine may fail via the piston hitting the head or the valves.

There are two main types of conrod that an engine designer can use, an 'I' section rod, like those used in all of the analysed engines and most bikes on the road, there is then a 'H' profile rod, this rod type tends to be used by performance car builders and is generally seen in motorcycles straight from the manufacturer.

Pistons tend to be cast as this is easy for aluminium as the temperature for it to become a liquid is much lower than steel, billet pistons are also quite common as an after-market choice, this is because they tend to be lighter. After market pistons also tend to be available with different top profiles to increase the compression ratio, therefor increasing the power output slightly.

All the cranks in the engines analysed were made of forged steel, all the conrods were also forged steel, the pistons were cast aluminium.

6.2 Balancing

During the operation of the engine several forces are generated by the motion of the crank, conrod, piston and pin, the largest being a so called first order inertial force, this force is caused by the movement of the piston pin and conrod. The purpose of crank balancing is to counteract the first order force.

When the vehicle is in use this first order force is the most easily felt, due to the frequency created by the motion of the reciprocating components it can be quite uncomfortable, this frequency is also a direct result of the RPM.

Using the equations for the inertia forces shown earlier the following graphs can be produced for a degree by degree inertia force plot. The major factors that changes the inertia force is the RPM the engine is running at and the mass of the components.

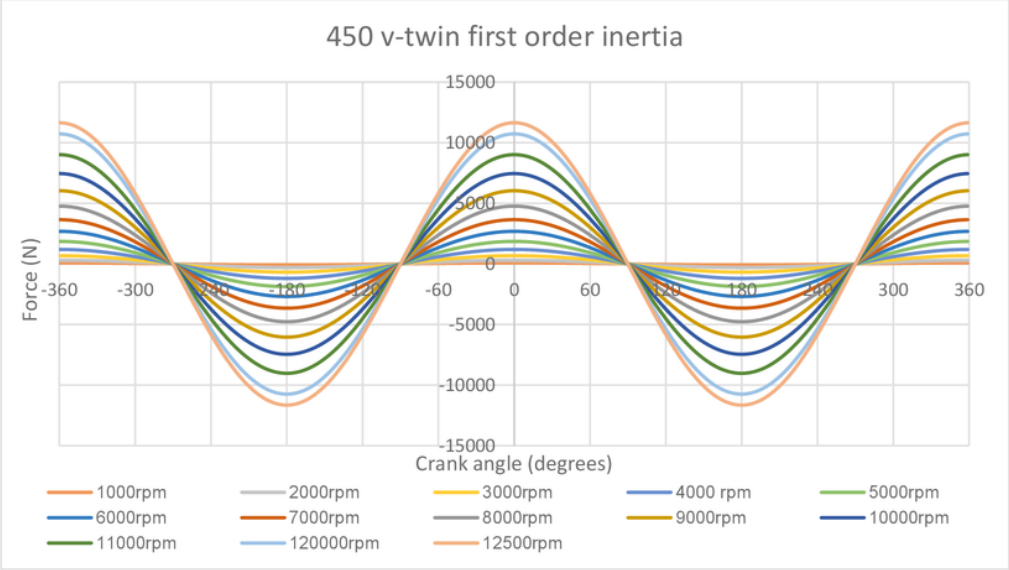


Figure 8 450 v-twin first order inertia

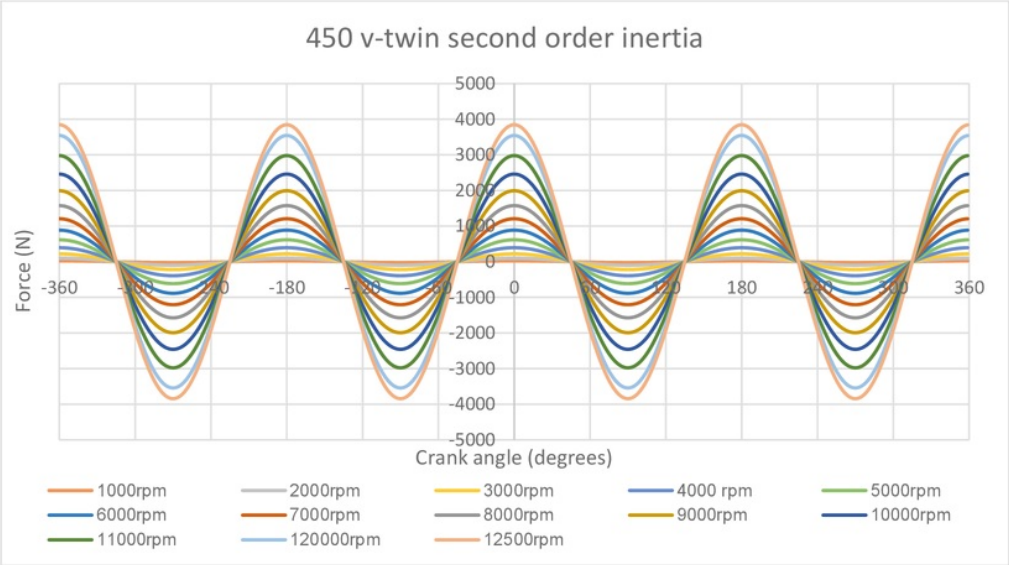


Figure 9 450 v-twin second order inertia

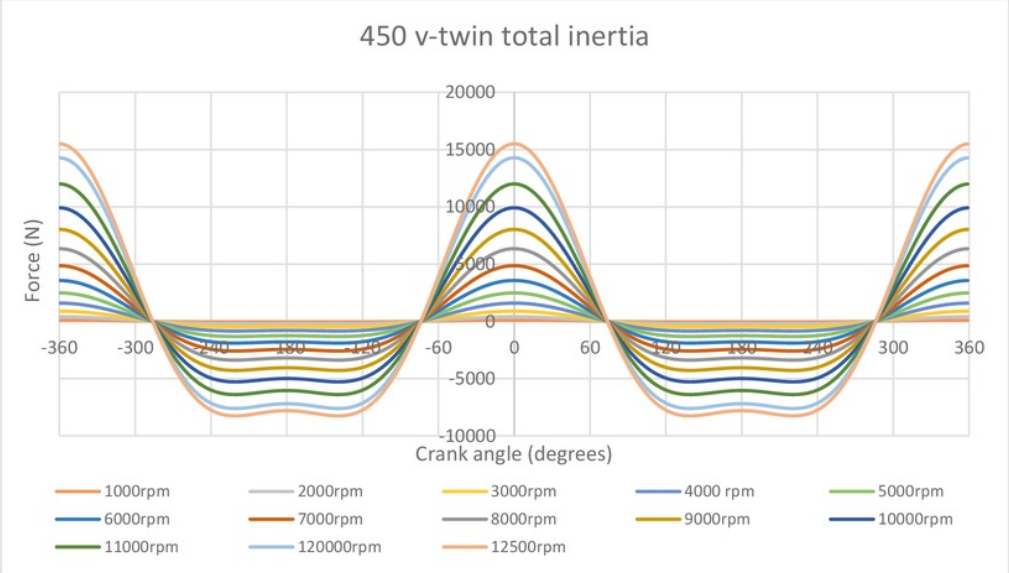


Figure 10 450 v-twin total inertia

As can be seen in figure 10 the inertia force reaches 15493 newtons, this is around half of the force generated during combustion so therefor is not something that can be easily disregarded, these 15493 newtons are important as this is the force that the conrod cap and bolts must cope with during operation, the gudgeon pin will also see some of this force but to a lesser degree.

Though not a focus here, the bolt strength should have close attention paid to it, as this could ultimately lead to failure problems in the future.

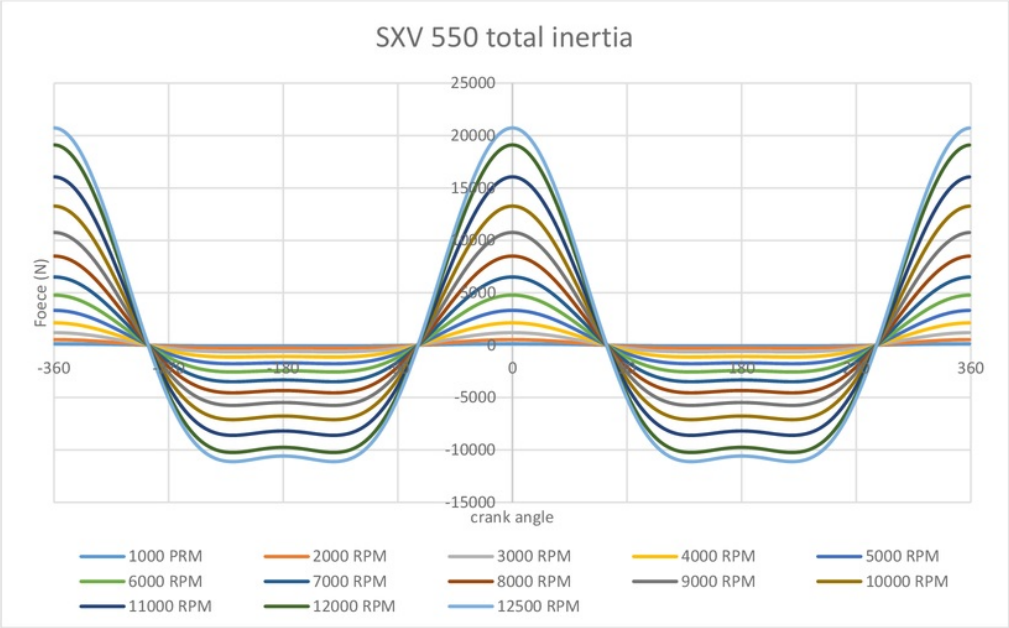


Figure 11 SXV550 total inertia

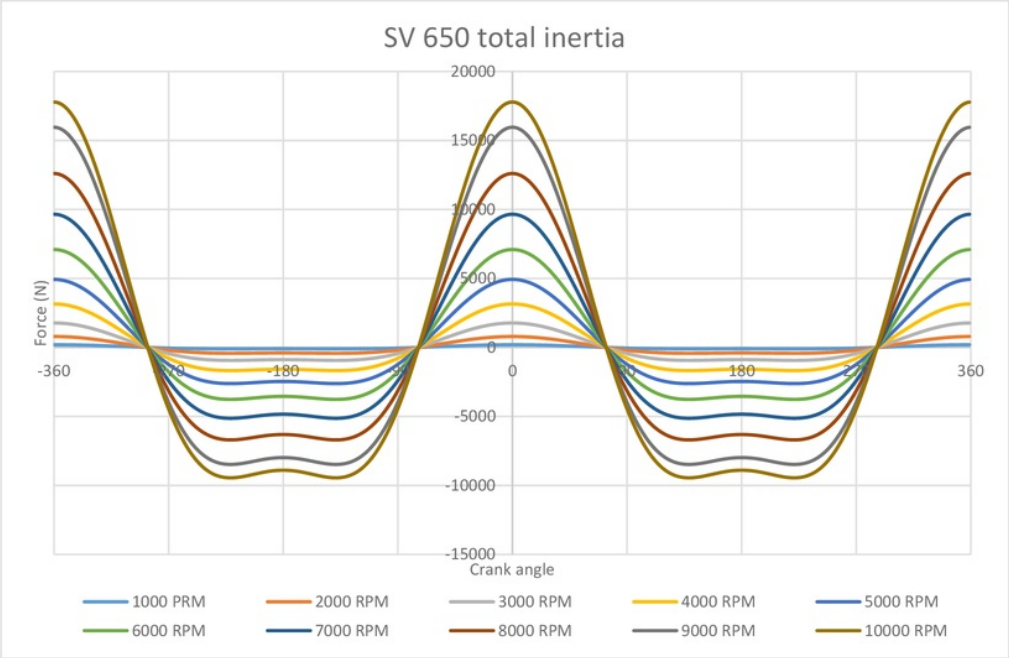


Figure 12 SV650 total inertia

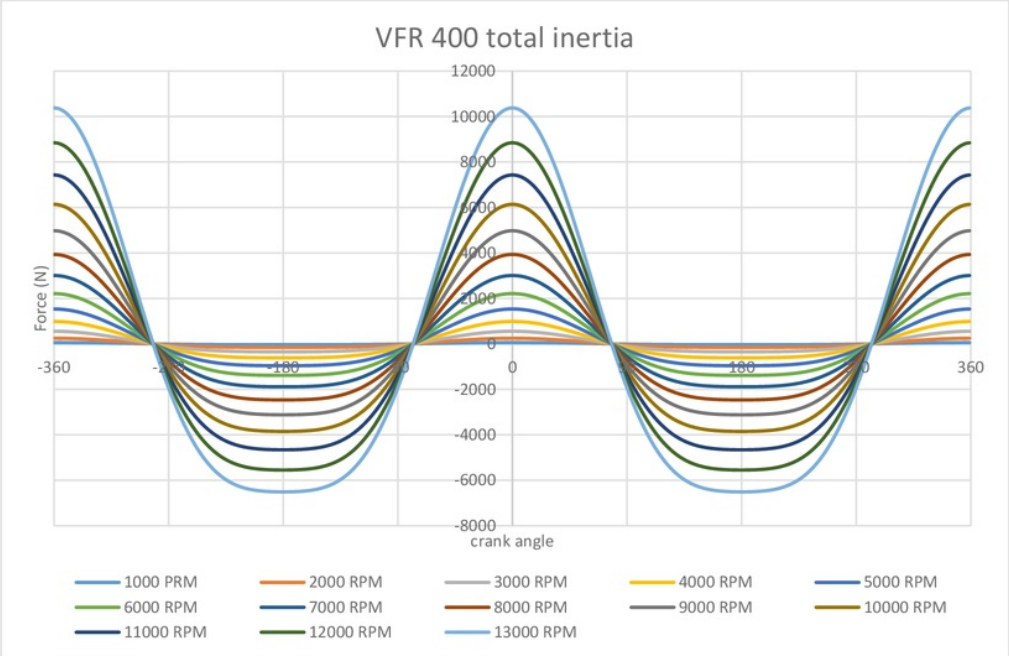


Figure 13 VFR400 total inertia

As can be seen in figure 11, 12 and 13 the SXV has the highest inertia force of all the analysed engines, this is in most part due to the high rpm that the engine can reach, though the VFR reaches a similar RPM the components are much lighter so it doesn't generate such a high force. The SV has the heaviest components of all three engines but doesn't rev as high as the other two, so therefore the inertia force doesn't get quite as high as the SXV.

7 FEA

During the process of creating the CAD models for the new engine, a feature of Solidworks was used to make the individual CAD models driven from an excel document, this enabled all of the separate models to change when a figure such as the mean piston speed of the max power RPM was change, this would also enable easy changes to the total engine displacement or the angle of the cylinders. Due to this method being used to drive all the major features of the CAD assembly it is extremely easy to completely change the engine without any troubles.

Once the overall model had been designed an FEA, or finite element analysis, could be carried out on the components of the assembly. The following section discusses the many different components of an FEA that need to be considered.

During the initial stages of the FEA the author found that it was imperative to simulate the oil film that forms between the journals and bearings during operation.

Oil is an extremely hard substance to simulate due to its nature of being a viscous liquid that changes it viscosity with heat, due to this changeability no software that is available to the author can simulate the oil film.

If the crank were to have no clearance between it and the conrods and the same with it and the crank case the numbers that would be generated would be artificially high, this would be cause for concern as the it would incite the need to make the whole system unnecessarily stronger.

Due to the damper systems offered in Solidworks not working in the expected way, the author decided to use a solid medium to simulate the oil, for this task a material with a very low young's modulus was needed, as such a rubber from the Solidworks library was selected. The thickness of the rubber was set a 0.005mm, this thickness choice is supported by the minimum oil film thicknesses given in the Mahle powertrain cylinder components book of 0.001mm. (Mahle GmbH, 2010)

The data set available from the triumph was an average for the three cylinders of the motorcycle, this meant using the same data set for both cylinders of the new engine, this is fine as it is to be expected that both cylinders would run exactly the same in perfect conditions.

A motion simulation, that is one of the features in Solidworks, was utilised to create the full simulation of the whole engine cycle, this feature requires quite a lot of setup in the form of mating all of the individual components together, creating contact conditions between each component and adding the required forces.

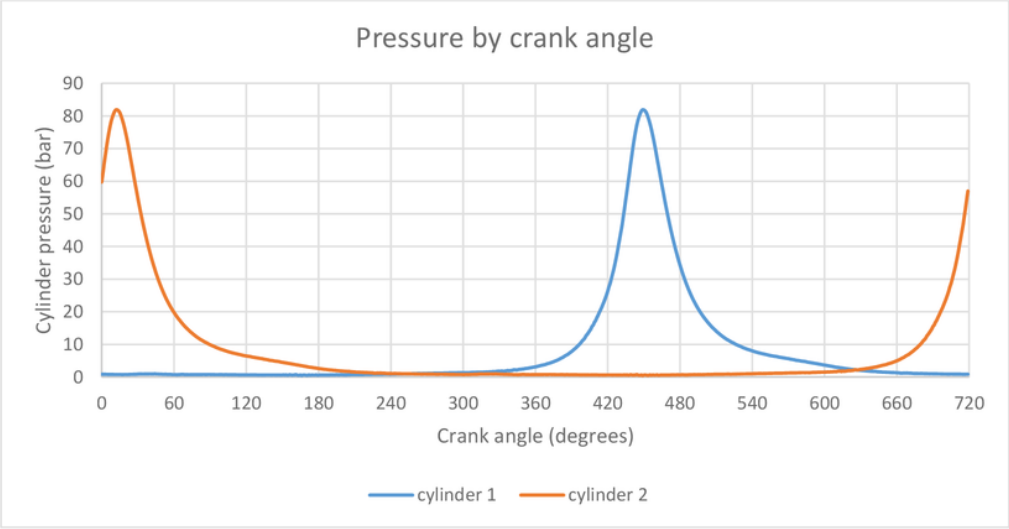


Figure 14 Pressure by crank angle

To transfer the data from excel to Soildworks the data points feature was used, this allowed a CSV file to be created and imported. This CSV file needed to be in terms of force and time, therefore the time taken for 2 revolutions of the engine needed to be calculated, this was done by dividing the RPM by 60, turning it into RPS, or rotations per second, then dividing one second by the resulting number.

$$time\ for\ 2\ revolutions = \left(\frac{1}{\left(\frac{RPM}{60}\right)}\right) \times 2$$

This time then needs to be paired with the available pressure data, the pressure data is dispersed over 720 degrees of crank rotation, this equates to 2 revolutions of the engine hence the doubling of the time.

The results of the CSV file imports can be seen in figure 15 and 16. The peak force for each cylinder is in a different place, this is due to the cylinders firing in different places throughout the cycle. For the designed engine the V angle of 80-degrees needs to be considered. If the engine were an inline twin, then the cylinder firing would be 360 degrees apart, if it were a 90-degree V-twin it would be 450-degrees, though for the engine designed it will be 440-degrees apart due to the 80-degrees V-angle.

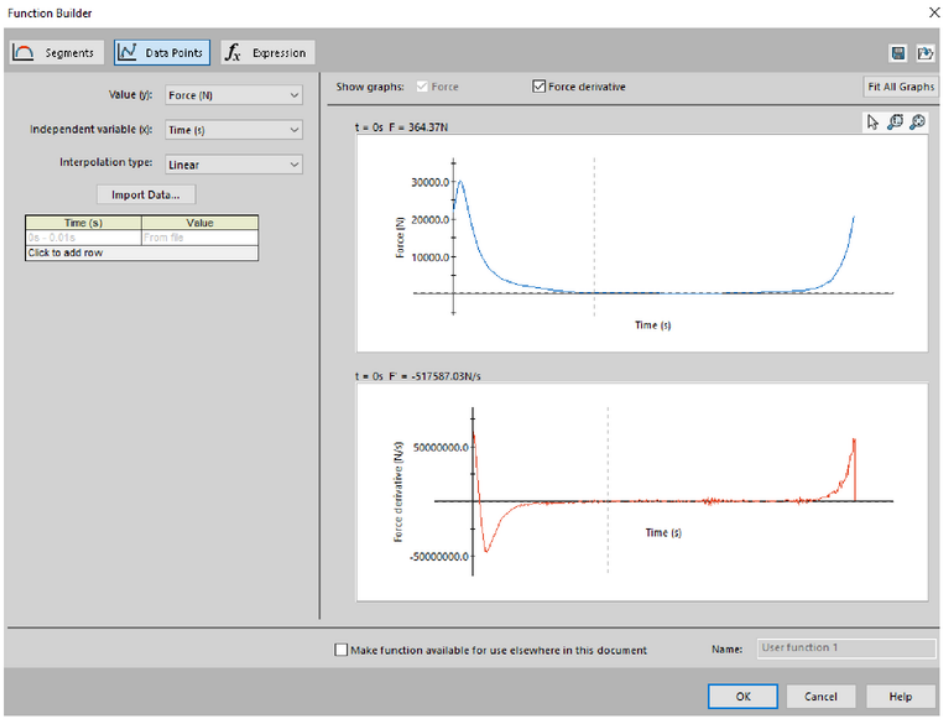


Figure 15 Cylinder 2 Solidworks data points plot

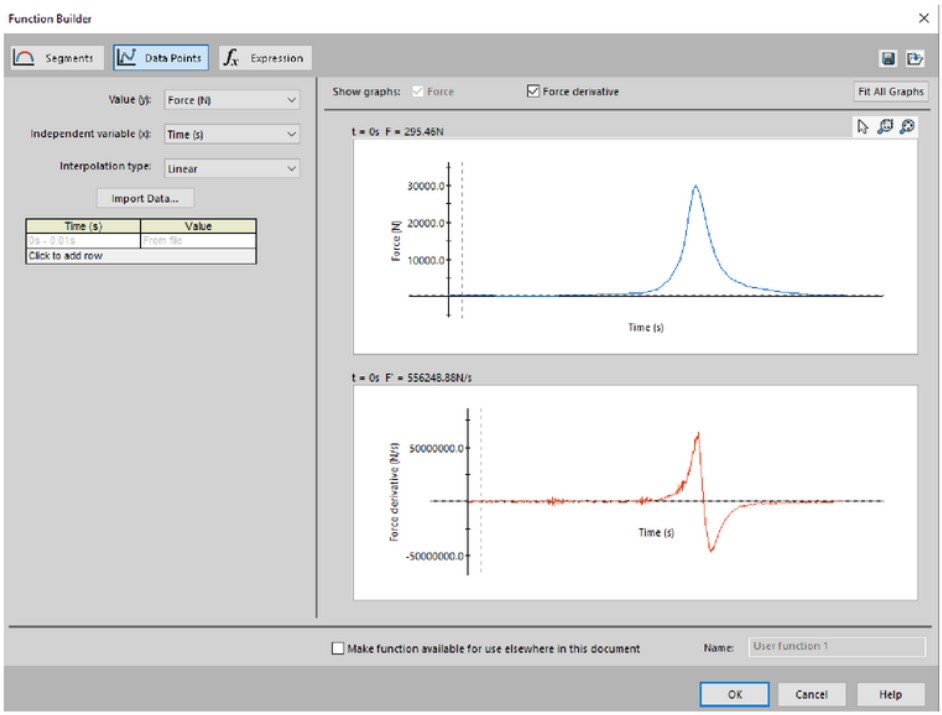


Figure 16 Cylinder 1 Solidworks data points plot

Solid body contacts were utilised for all the areas of contact between the different components, this feature allows for the selection of different friction coefficients.

To lessen the amount to time it took for the FEA to solve the decision was made to reduce the number of complex features, mainly the fillets that have no impact on the strength of the crank.

7.1 Mesh

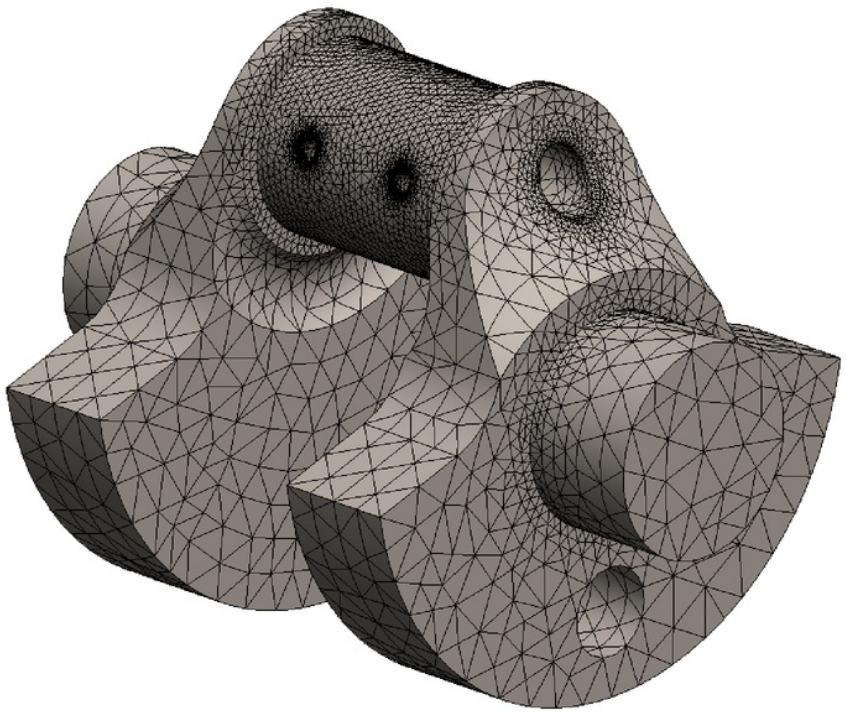


Figure 17 Meshed crank

Figure 17 shows the fully meshed crank with the minimal mesh control that Solidworks offers, the mesh control offers the option to make the mesh in certain area denser, for this application this option is extremely beneficial as there is no need to have a high element count around areas of no stress, it also helps in keeping the calculation time down.

If no mesh control was applied there would be an evident lack of detail once the FEA had been carried out, this would pose problems for the final results as there would either be much too high or much to low figures, the standard element size used on the crank was 6mm, this is adequate for most of the crank, but not the areas of interest around the journal transitions. (manning, 2012)

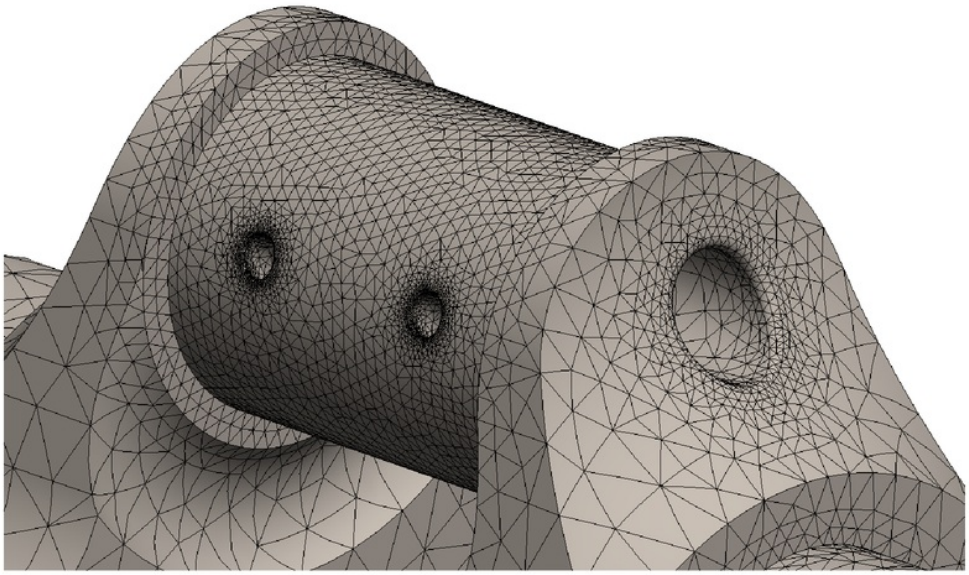


Figure 18 close view of big end journal and oil hole meshing

Figure 18 shows in better detail the mesh control, the mesh used in the areas of interest was taken down to a size of 1.5mm, this could have been taken down even further but the amount of time to solve goes up exponentially with element count, so was therefor the 1.5mm element size was deemed adequate.

The biggest limitation of the mesh control in Solidworks is that there is no individual element control, this means that meshes can be chaotic, due to this non uniformity errors could be caused and therefor results skewed.

A more suitable mesh to use on a crank could be a brick type mesh, as much more control can be had over these, they also have many less calculations associated with them so the solve time of an FEA would decrease greatly.

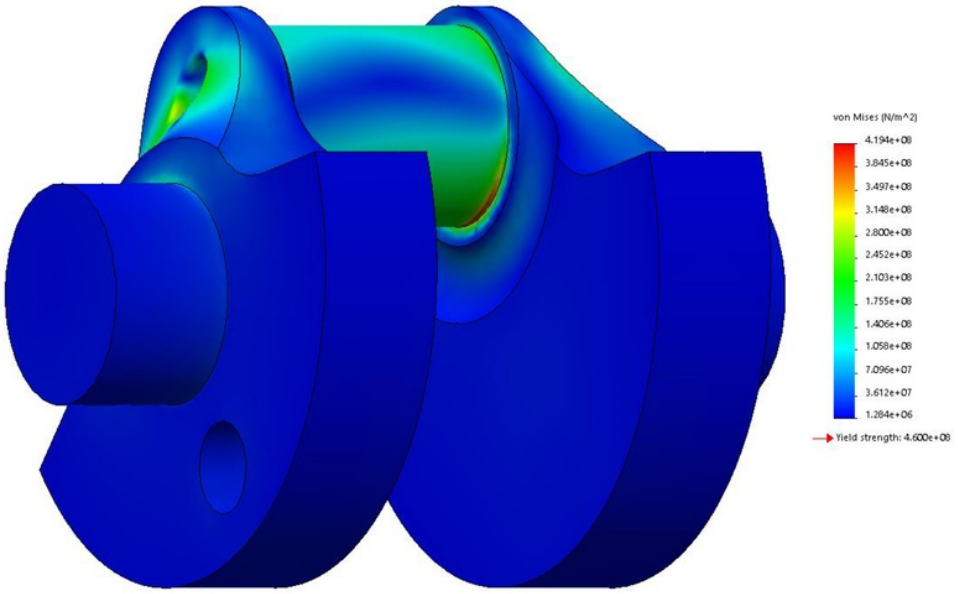


Figure 19 FEA stress concentration, compressive zone (von mises stress)

As can be seen in figure 19 there is a small in area but significant in magnitude stress concentration where the big end journal transitions to the crank web, this is an expected place for this to appear and is confirmed in multiple other papers looking at crank FEA. (Suraj K. Kolhe, 2016) (MENG Jian, 2010) (Gu Yingkui, 2011) (Lucjan Witek, 2017) (K.Dilip kumar, 2017)

This stress concentration reaches a maximum of 416KN/M^2 which is close to the yield of the selected AISI 4130 steel, whose yield is 460KN/M^2. This could cause problems with the overall life of the part, one possible way around this is to use another common crank steel, AISI 4340, this steel has a yield of 710KN/m^2, this is much more appropriate for a performance crankshaft such as this. An FEA was carried out with this newly selected material but there were no discernible changes due to most of the steel properties being the same, such as the young's modulus.

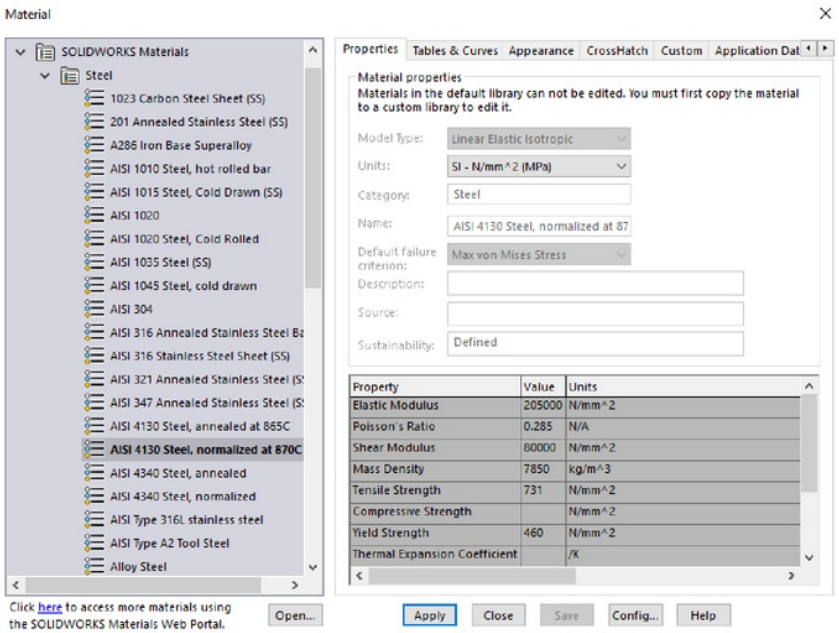


Figure 20 4130 steel material selection in Solidworks

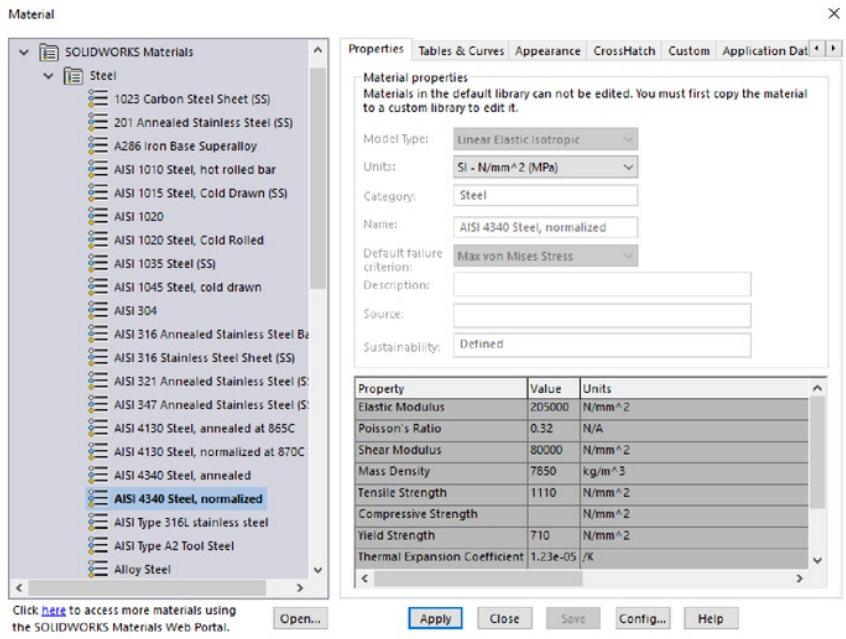


Figure 21 4340 steel material selection in Solidworks

Figure 20 and 21 show the two different materials that the author used in the FEA, the data show is what the Solidworks library hold for each of them, this is deemed to be correct.

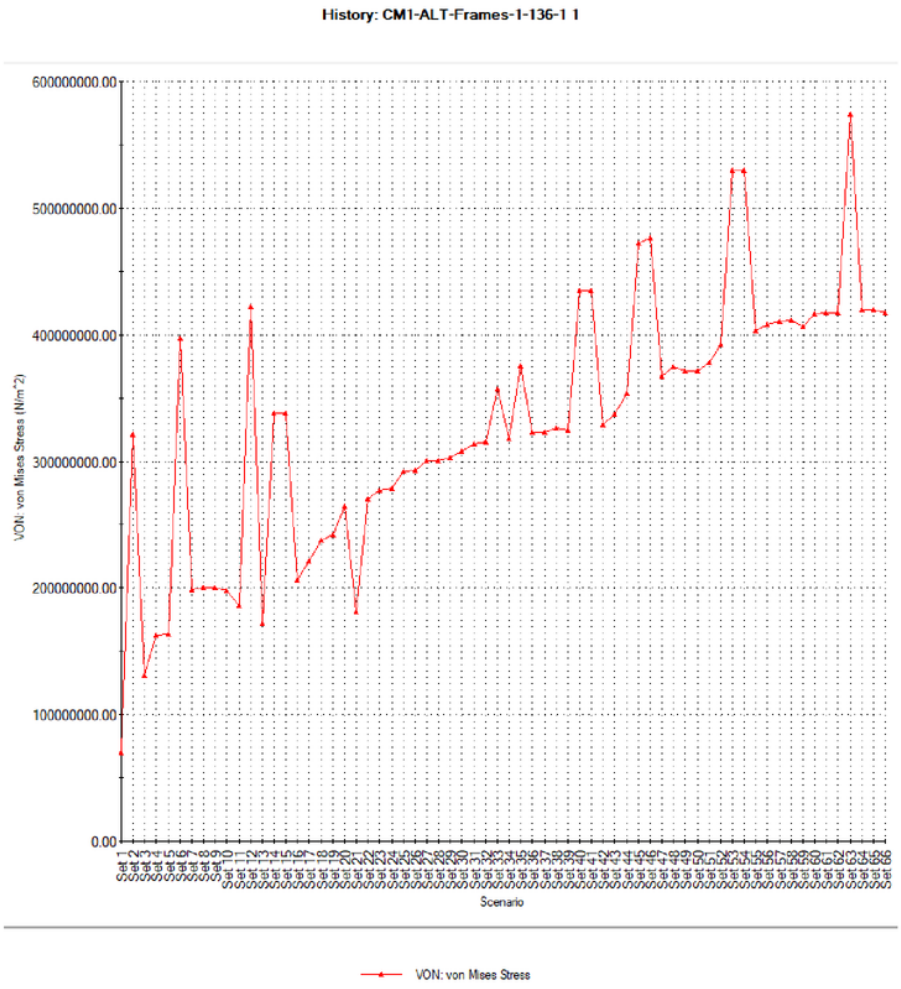


Figure 22 Von Mises stress plot

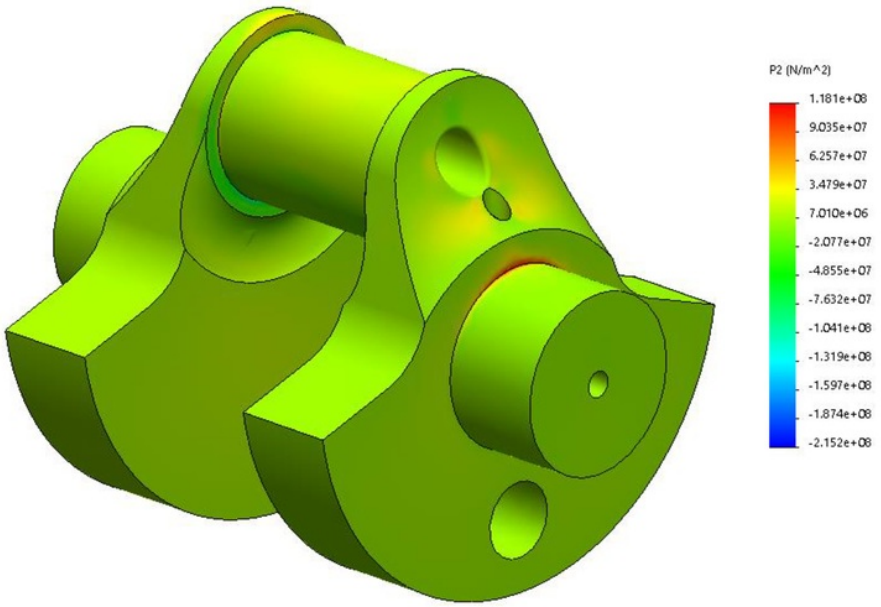


Figure 23 FEA stress concentration, tensile zone (2nd principal stress)

In figure 23 there is a small zone with a noticeable tensile force, this was to be expected, as this is another spot which would be most affected by the flex in the crank, this matches results show by several other papers, this force is much lower in magnitude than the compressive force seen in figure 19, this may be due to the main journal being 1.3 times larger than the big end journal, therefor the stress has a larger area to disperse itself over.

The force shows at 181KN/M^2, this is much lower than the yield of the material. This point may not be the highest tensile load throughout the cycle but due to issues with Soildworks this point is currently the highest plausible figure available.

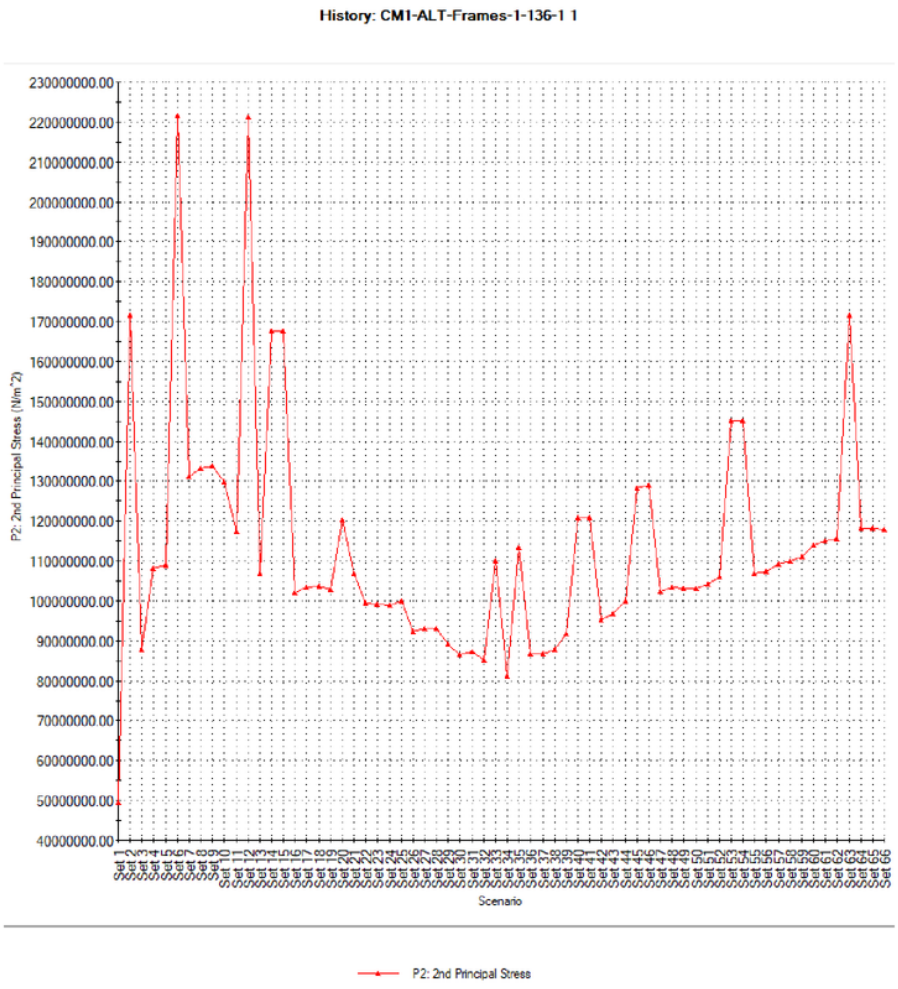


Figure 24 Second principal stress plot

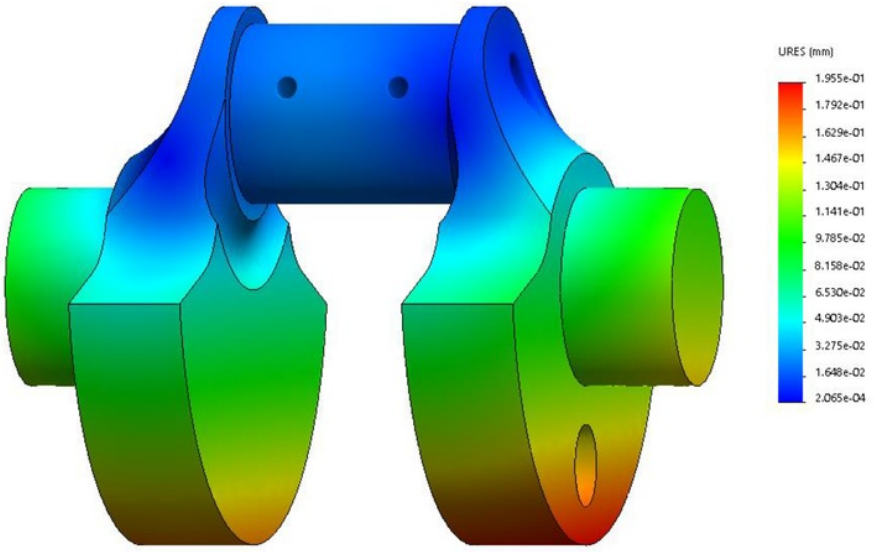


Figure 25 FEA Displacement

In figure 25 there is only a small amount of flex in the crank at the peak of combustion pressure, around 0.19mm, this also only occurs at the outmost point of the crank web. This deflection shouldn't be a problem as it is at the furthest point from the journals. Lookint at the bigend journal there is little to no flex at all, this would mean that the crank is corectely sized.

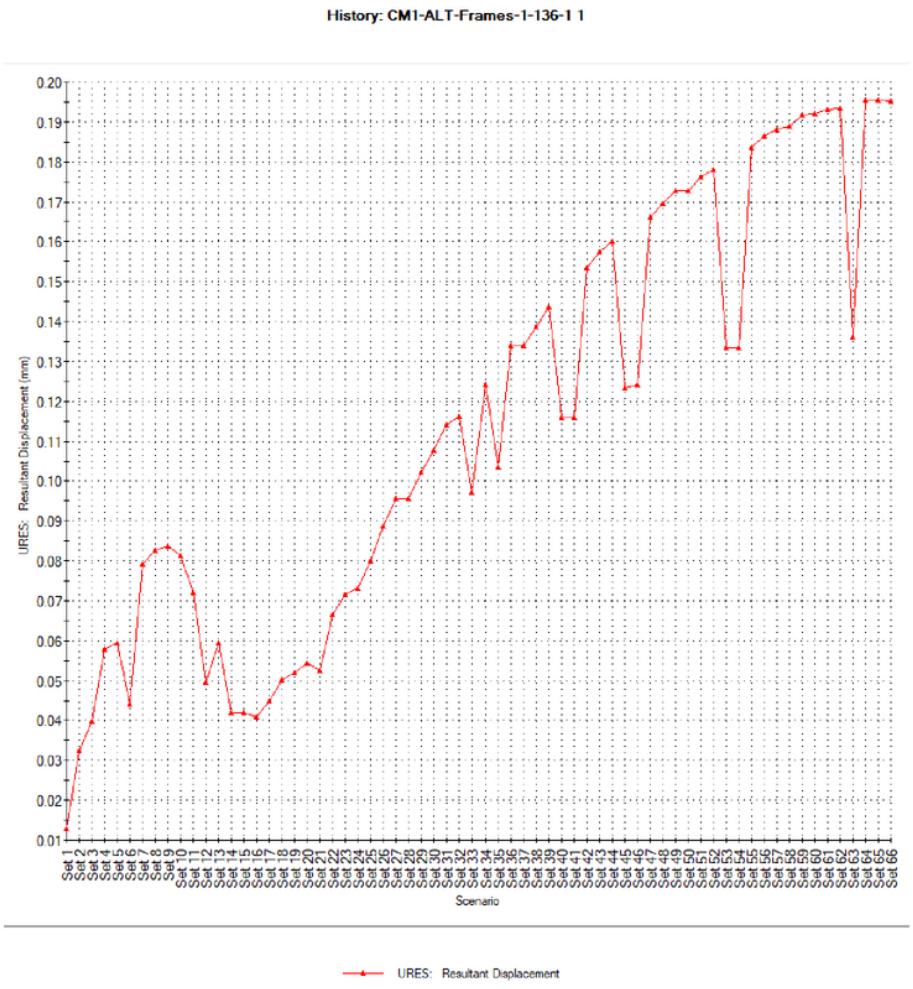


Figure 26 Displacement plot

A point of notice that can be seen throughout the data are the erroneous spikes in the plots generated by Soildworks from the FEA data, it is as yet unknown why these deviations from the trend are occurring, it is known that it has something to do with either the motion simulation itself or the transfer of motion data over the individual part, it may also be attributable to the student licence for Solidworks limiting the software package or possible hardware limitations.

Of the 400-500 data sets created in the motion simulation by Solidworks, on numerous occasions, it would only export a very limited number, this may be due to the complexity of the FEA carried out or possibly the student licence limiting the software.

Though Solidworks student is adequate it is certainly is not the best to carry out a complicated FEA such as this. Programs such as ANSYS or one of the software packages produced by Altair would be much more productive.

The conrod would have been run through an FEA but due to limitations that may be the result a student licence for Solidworks the methods used for the simulation could not be applied to the conrod.

8 Balance shafts

The purpose of a balance shaft is to cancel out the second order forces generated by the motion of the internal components of the engine. This force is considerably smaller than the first order being around a third of the force, as seen in figure 8 and 9.

A balance shaft must turn opposite the rotation of the crank at twice the velocity, the rotation of a balance shaft is to counteract the forces seen in figure 9.

The need for a balance shaft is worked out by calculating the vectors that the first and second order force vectors act at. When analysing a 90-degree v-twin it is apparent that the vectors cancel each other out so therefor there is no need for a balance shaft. When the angle of the V deviates from 90-degrees there is then a need for a balance shaft.

When a 90-degree v twin is examined for vectors it can be seen that the two forward vectors of the system are along arrow 2 in figure 27, the accompanying first reverse vector is then found to be opposite of arrow two but still in the same location, the second reverse vector is opposite arrow 3, this is due to the reverse vector being the same angle behind arrow 1 as the first reverse vector is in front. The following equations prove that all the first order forces cancel each other.

$$Reverse1 = Reverse2 = \frac{M_{rec}}{2} \times R \times \omega^2$$

$$Forward1 = Forward2 = \frac{M_{rec}}{2} \times R \times \omega^2$$

When the v angle changes from 90-degrees the reverse vectors no longer line up with each other and therefore do not cancel each other out. When this is the case vectors need to be resolved for vertical and horizontal forces.

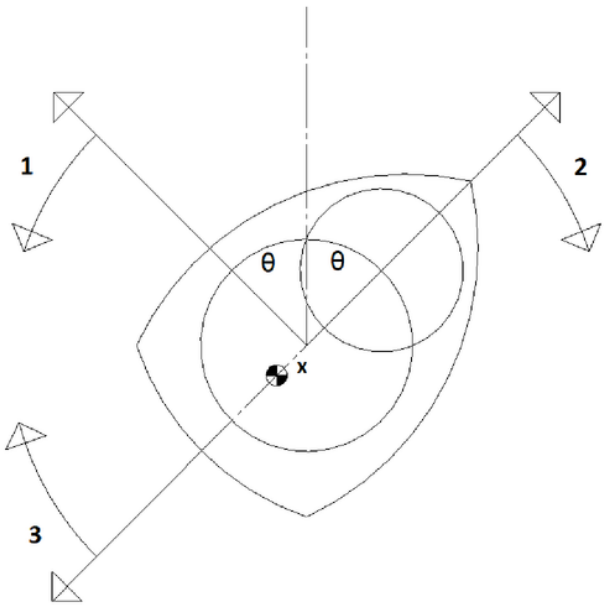


Figure 27 vectors diagram

To work out the CoG offset of the balance shaft the following equation was used, this method requires the user to define a weight of the balance shaft, this method can be useful if the weight is being kept to a minimum.

$$Y = \frac{M_{rec}}{2} \times R \times M_{bal}$$

This equation can also be rearranged to work out a mass for the balance shaft instead, though this method requires the user to specify a Cog offset, this method could be used of there was a shortage of space available.

$$M_{bal} = \frac{\frac{M_{rec}}{2} \times R}{Y}$$

Though the SXV engine is a 77-degree v it does not have a balance shaft, this could be because it is a race motorcycle and is trying to keep weight to a minimum. Though in the authors experience the motorcycle was smooth regardless.

The designed engine has an 80-degree v angle therefor it would need a balance shaft, using the equations above the balance shaft would need either a weight of 1.36Kg at a CoG of 1.36mm.

8.1 Vector calculations for a single cylinder

$$1 = \frac{M_{rec}}{2} \times R \times \omega^2$$

$$2 = \left(M_{rot} + \frac{M_{rec}}{2}\right) \times R \times \omega^2$$

$$3 = (M_{rot} + M_{rec}) \times R \times \omega^2$$

$$resultant\ vertical\ force = \frac{M_{rec}}{2} \times R \times \omega^2 \times \cos\theta + \frac{M_{rec}}{2} \times R \times \omega^2 \cos\theta$$

$$resultant\ vertical\ force = M_{rec} \times R \times \omega^2 \times \cos\theta$$

$$resultant\ horizontal\ force = \frac{M_{rec}}{2} \times R \times \omega^2 \times \sin\theta - \frac{M_{rec}}{2} \times R \times \omega^2 \times \sin\theta = 0$$

9 Centre of gravity

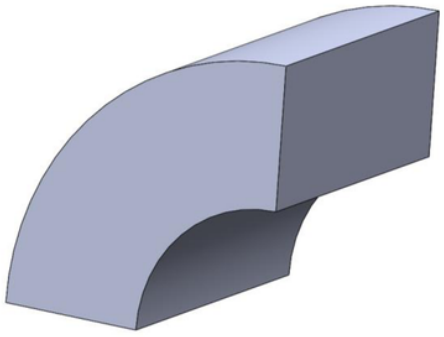


Figure 28 90-degree semicircle segment

During the process of finding the CoG of the balance shaft the avenue of a mathematical solution was explored, this mathematical exploration ultimately ended in failure, giving the CoG of a triangle, more research could most definitely be done but due to time constraints this is not done here. Due to this failure the author decided to pursue an avenue using polynomials instead.

The author used Solidworks to generate the shape seen in figure 28. Using two different base diameters, 20mm in figure 29 and 40mm in figure 30 many results were recorded to create a polynomial for each of the two diameters, these polynomials could then be used to work out where the CoG would theoretically fall. Both polynomials generated had

a deviation of around half of a millimetre above and below where the real CoG is, due to this deviation the polynomials could only be used as a guide and if more accuracy is needed then a part should be created and analysed.

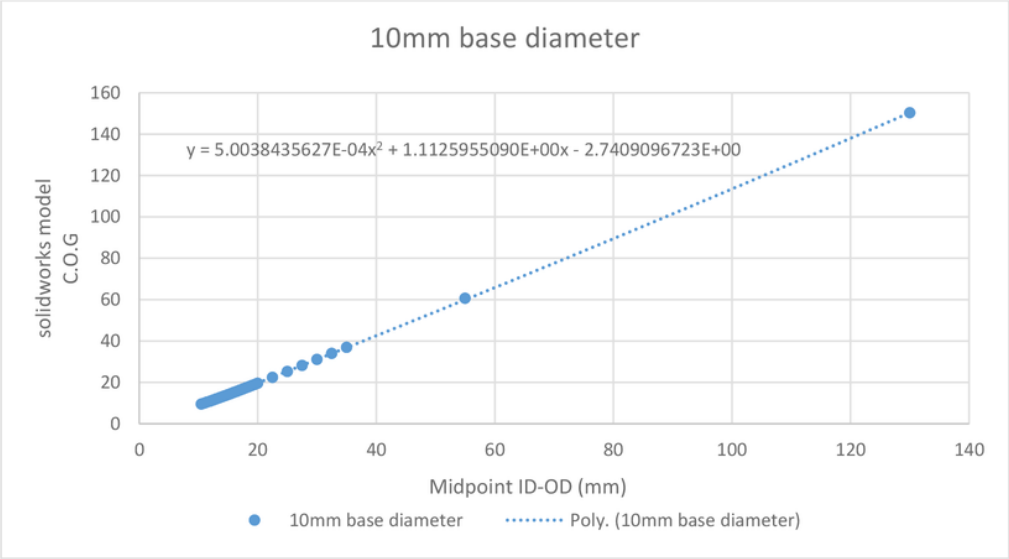


Figure 29 COG polynomial plot 10mm base

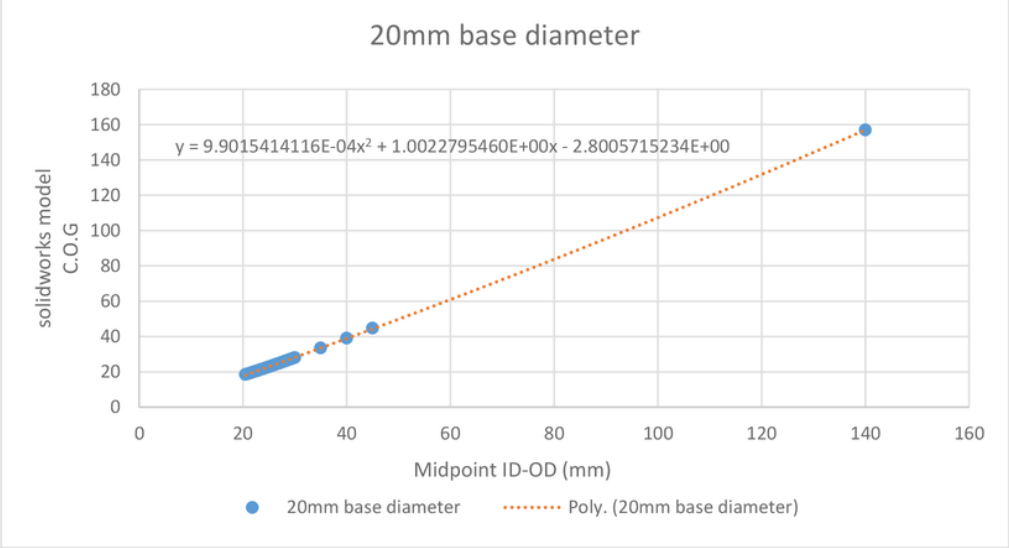


Figure 30 COG polynomial plot 20mm base

10 Metal treatments

All types but a few types of metal can be subject to some form of surface treatment process, whether it is using chemicals or heat. There are some surface treatments that are used with engine components, nearly all of which involve high temperatures. Most surface treatments do not add any extra mass to the component so are extremely beneficial in that regard, the main down sides of surface treatments are cost and time.

10.1 Induction hardening

Induction hardening it one such use of high temperature treatments; it uses a copper coil placed around the area to be heated and then applies an electric current which causes a magnetic field that excites the particles in the area contained within the coil, this then rapidly heats the contained area up to temperatures above 700 Celsius, the part is then left to cool naturally, this initiates the formation of certain crystalline structures, depending on the amount of carbon in the material different structures form, as seen in figure 31.

These structures cause the surface to become much harder than they were before, this lets the affected area see much higher surface pressure before failure, it also increases the wear life of the area treated.

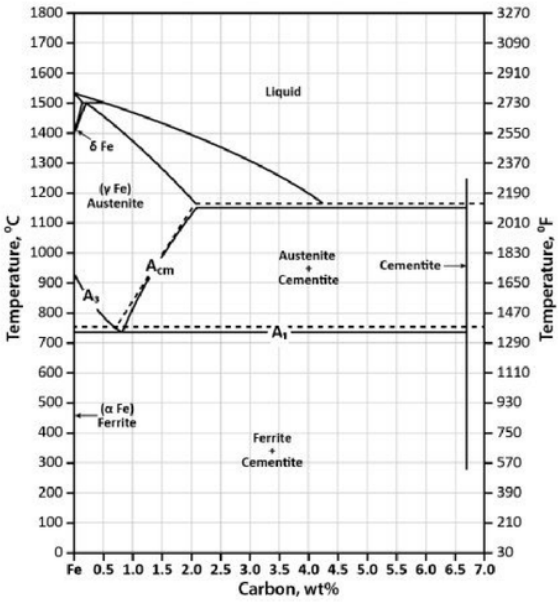


Figure 31 steel phase diagram (Industrial Metallurgists LLC, 2019)

10.2 Pulse plasma nitriding

With pulse plasma nitriding parts are placed into a chamber that has a nitrogen rich atmosphere which is heated electrically to produce plasma, the parts are then cycled through heat and cooled states, the amount of cycles depending on permeation depth required. The result of nitriding is that the surface is harder than the original material, in some cases double, this give the part the ability to take much higher loads than originally designed for. (northeast coating, 2019)

10.3 shot peening

Shot peening is the process of shooting small beads of a steel medium at the surface that is being treated, this introduces a compressive stress over the area that has been treated, this extra compressive residual stress is on top of the existing normal residual stress left from manufacturing. (Curtiss-Wright , 2019)

10.4 diamond like coat

Diamond like carbon or DLC is a another surface treatment that is common in new engines, though usually used on gudgeon pins the application to the surface of big end journals of a crank may work just as well, the treatment is a microns thick layer of carbon which reduces the friction coefficient of the surface. (Robertson, 2002)

Adding different surface finish techniques into Solidworks would be close to impossible as surface treatments are usually zonal and not homogeneous throughout the part, Solidworks does not contain the capability to assign materials in a zonal fashion, to do this in Solidworks the whole material would need to be changed there for changing the whole characteristic of the part. This would then yield incorrect FEA results as the internal structure would be much stronger than a real pert would.

11 Further work

11.1 Head model

The author had wanted to create a working model of the head and valve train but stopped due to time constraints. This model would have included the valves, valve springs, spring retaining collets, cams and the head itself. This head model would also need include a cam profile, this cam profile could then be accompanied by a fuelling map, this could then lead to finding the theoretical power output of the engine.

11.2 Engine cases and gearbox

Another part that would be vital to a full model engine is the rest of the running gear in the engine. This would include the clutch, gearbox and the rest of the bearings. An oiling system could also be designed, this would need to include pumps, ducts and a coupling to the end fed crank.

11.3 Friction model

From all the work done and the further work that could be carried out a friction model for the whole engine could be made, this would enable a figure for frictional losses to be produced and in conjunction with a theoretical power output a possible rear wheel horsepower could be gained.

12 References

Curtiss-Wright . (2019, 04 27). *Shot Peening*. Retrieved from Curtiss-Wright : https://cwst.com/shot-peening/overview/

Gu Yingkui, Z. Z. (2011). Strength Analysis of Diesel Engine Crankshaft Based on PRO/E and ANSYS. *2011 Third International Conference on Measuring Technology and Mechatronics Automation* (p. 364). IEEE.

Industrial Metallurgists LLC. (2019, 04 27). *Phase Diagram - Industrial Metallurgists*. Retrieved from Industrial Metallurgists LLC: https://www.imetllc.com/training-article/phase-diagram/

K.Dilip kumar, P. D. (2017). Structural and Dynamic Analysis of Six Cylinder Four Stroke Diesel Engine Crank Shaft Subjected to Various Loading Conditions. *International Journal of Latest Engineering Research and Applications*, 32-35.

Lucjan Witek, M. S. (2017). Stress and failure analysis of the crankshaft of diesel engine. *Engineering Failure Analysis 82*, 710-711.

Mahle GmbH. (2010). Cylinder components. In M. GmbH, *Cylinder components* (p. 93).

manning, J. (2012). Internal combustion engine design. In J. manning, *Internal combustion engine design* (pp. 320-327). Shoreham-by-sea: Ricardo UK limited.

MENG Jian, L. Y.-q.-x. (2010). Intension Analysis of 3-D Finite Element Analysis on 380 diesel crankshaft. *2010 International Conference on Computational and Information Sciences* (p. 1271). IEEE.

motorcyclespecs. (2019, 04 27). *Aprilia SXV 550*. Retrieved from motorcyclespecs: https://www.motorcyclespecs.co.za/model/aprilia/aprilia_sxv550%2008.htm

motorcyclespecs. (2019, 04 27). *Honda VFR 400*. Retrieved from motorcyclespecs: https://www.motorcyclespecs.co.za/model/Honda/honda_vfr400r%2087.htm

motorcyclespecs. (2019, 04 27). *Suzuki SV 650*. Retrieved from motorcyclespecs: https://www.motorcyclespecs.co.za/model/suzu/suzuki_sv650s_01.htm

northeast coating. (2019, 04 27). *Plasma Nitriding Hardness Chart*. Retrieved from northeast coating: www.northeastcoating.com/products/plasma-nitriding/hardness-chart

Robertson, J. (2002). Diamond-like amorphous carbon. *Materials Science and Engineering*.

simonevans. (2019, 04 27). *Honda VFR400 NC30*. Retrieved from simonevans: http://www.simonevans.co.uk/v-four/vfr400.htm

Suraj K. Kolhe, P. G. (2016). Diesel Engine Crankshaft High Cycle Fatigue Life Estimation and Improvement Through FEA. *International Journal of Engineering Research & Technology (IJERT)*, 551-553.

thecunningham. (2019, 04 27). *SXV pistons*. Retrieved from apriliaforum: https://www.apriliaforum.com/forums/showthread.php?261318-SXV-pistons